The Strain Rate Dependence of Shear Viscosity, Pressure and Energy from Two-Body and Three-Body Interactions

Gianluca Marcelli, B.D. Todd, and Richard J. Sadus

Centre for Molecular Simulation and School of Information Technology, Swinburne University of Technology, PO Box 218, Hawthorn, Victoria 3122, Australia

Email: BTodd@swin.edu.au, RSadus@swin.edu.au

Keywords: Theory, non-equilibrium molecular dynamics, shear viscosity, xenon

Abstract

Nonequilibrium molecular dynamics simulations are reported for the shear viscosity of xenon using accurate two- and three-body potentials. The dependence of the hydrostatic pressure, and energy are observed to vary linearly with the square of the strain rate. This is contrast to the non-analytic three-halves power dependency on strain rate predicted by mode coupling theory. This result is attributed solely to the two-body potential. The main effect of the three-body potential is to alter the magnitude of the pressure, energy and viscosity profiles.

1. Introduction

Recent [1] non-equilibrium molecular dynamics simulation (NEMD) results for argon, using the Barker-Fisher-Watts (BFW) [2] and Axilrod-Teller (AT) [3] intermolecular potentials, indicate that both pressure and energy varies linearly with the square of the strain rate. In contrast, mode coupling theory [4] predicts a non-analytic three halves power dependency on the strain rate. Most earlier molecular simulation studies [5-7] using effective multi-body intermolecular potentials such as the Lennard-Jones or Weeks-Chandler-Anderson (WCA) intermolecular potentials appear to support the predictions of mode coupling theory. Other results [8,9] for argon using the BFW and AT potentials also indicate a three-halves dependence on strain rate. Ryckaert et al. [10] reported a stain rate-squared dependence of the shear viscosity but the significance of these results is unclear because of the high strain rates and large statistical uncertainties in the data [11] and the possible influence of string-phases [12,13]. In contrast, our results [1] for argon were obtained with greater statistical accuracy and no string phases or other sources of error were observed.

It is of considerable interest to determine whether or not our results for argon are also valid for other atoms. In this work, we report NEMD calculations for the shear viscosity of xenon. Xenon was chosen because it is considerably larger than argon; an accurate two-body potential [14] is available in the literature and the non-additive coefficient is known accurately [15]. To the best of our knowledge, the shear viscosity of xenon has not been reported previously using accurate two- and three-body intermolecular potentials. The results reported here indicate that both energy and pressure have an unambiguous dependency of the strain rate-squared.

2. Theory

The details of the simulation have been discussed extensively elsewhere [1]. Therefore, only an outline of the main details is given here.

2.1. Intermolecular potentials

The total intermolecular potential (ϕ) is a contribution from two-body interactions ($\phi^{(2)}$) and three-body dispersion interactions (ϕ^{3BDisp}):

$$\phi(r) = \phi^{(2)}(r) + \phi^{3BDisp}(r) \tag{1}$$

Several accurate two-body potentials are available in the literature [16] and a recent review is available [17]. For xenon, Barker et al. [14] reported the following accurate two-body potential:

$$\phi^{(2)}(r) = \phi_0(r) + \phi_1(r) \tag{2}$$

where $\phi_0(r)$ is:

$$\phi_0(r) = \varepsilon\left[\sum_{i=0}^{5} A_i (x-1)^i \exp\left[\alpha(1-x)\right] - \sum_{j=0}^{2} \frac{C_{2j+6}}{\delta + x^{2j+6}}\right] \tag{3}$$

and

$$\phi_1(r) = \begin{cases} \left[P(x-1)^4 + Q(x-1)^5\right]\exp\left[\alpha'(1-x)\right] & x > 1 \\ 0 & x \le 1 \end{cases} \tag{4}$$

In Eqn (3), $x = r/r_m$ where r_m is the intermolecular separation at which the potential has a minimum value and the other parameters are obtained by fitting the potential to experimental data for molecular beam scattering, second virial coefficients, and long-range interaction coefficients. The contribution from the repulsion term has an exponential-dependence on intermolecular separation and the contribution to dispersion of the C_6, C_8 and C_{10} coefficients are included. In Eqn (4) α', P and Q are additional parameters obtained by fitting data for scattering differential cross-sections. For this work we have used the intermolecular parameters from the literature [14].

There are many possible contributions to three-body dispersion interactions [18,19]. However, recent work [18,20] has clearly established that there is a large degree of cancellation between the contributions and that the triple-dipole alone is an accurate representation of three-body dispersion interactions. The triple-dipole potential was evaluated from the formula proposed by Axilrod and Teller (AT) [3]:

$$\phi_{DDD} = \frac{v_{DDD}\left(1 + 3\cos\theta_i \cos\theta_j \cos\theta_k\right)}{\left(r_{ij} r_{ik} r_{jk}\right)^3} \tag{5}$$

where v_{DDD} is the non-additive coefficient, and the angles and intermolecular separations refer to a triangular configuration of atoms. The non-additive coefficient for xenon (5573 a.u.) was taken from the literature [15].

2.2. NEMD Simulation Details

The NEMD simulations were performed by applying the standard SLLOD equations of motion for planar shear flow [12], using a Gaussian thermostat multiplier

to keep the kinetic temperature of the fluid constant. The pressure tensor of the fluid was calculated by the standard Irving-Kirkwood [21] expression, modified to include 3-body contributions [1]. The shear viscosity (η) was subsequently obtained from the off diagonal components of pressure tensor (P_{xy}, P_{yx}) and the strain rate ($\dot{\gamma}$) via relationship $\eta = -(P_{xy} + P_{yx}) / 2\dot{\gamma}$.

The equations of motion are integrated by a 5th order Gear predictor-corrector scheme [22], with a reduced integration time step ($t^* = t\sqrt{\varepsilon / m\sigma^2}$) of 0.001. A single nonequilibrium simulation trajectory is typically run for 250000 time steps. Averages are taken over 2 independent trajectories, each starting at a new configuration. To equilibrate the system, each trajectory is first run without a shearing field. After the shearing field is switched on, the first 50000 time steps of each trajectory are ignored, and the fluid is allowed to relax to a nonequilibrium steady-state. Thus, every pressure, energy and viscosity data point represents a total run length of $2 \times 200000 = 4 \times 10^5$ time steps.

A total system size of 500 atoms was used. The two-body potential was truncated at half the box length and appropriate long range correction terms were evaluated to recover the contribution to the pressure and energy for the full intermolecular potential [2]. Some care needs to be taken with the three-body potentials because the application of a periodic boundary can potentially destroy the spatial-invariance of three particles [18,23]. For a system size of 500 or more atoms, at the liquid density studied, truncating the three-body potentials at intermolecular separations of a quarter of the length of the simulation box was observed to be an excellent approximation to the full potential. This also avoided the problem of three-

body invariance to periodic boundary conditions. The long range corrections were determined as detailed elsewhere [1].

3. Results and Discussion

The results of NEMD simulations for the pressure, energy and shear viscosity of xenon at different strain rates are reported in Table 1. The normal convention was adopted for the reduced density ($\rho^* = \rho\sigma^3$), temperature ($T^* = kT/\varepsilon$), energy ($E^* = E/\varepsilon$), pressure ($P^* = P\sigma^3/\varepsilon$), viscosity ($\eta^* = \eta\sigma^2 / \sqrt{m\varepsilon}$) and strain rate ($\dot{\gamma}^* = \dot{\gamma}\sigma\sqrt{m/\varepsilon}$). Unless otherwise stated, all quantities quoted in this work are in terms of these reduced quantities and the superscript * will be omitted. All simulations were performed at the state point (ρ, T) = (0.6 [2.222 gcm^{-3}], 0.9 [252.9 K]). This point was chosen because it is representative of the liquid phase of xenon being approximately mid-way between the triple point and the critical point

The uncertainties in the time averages for the energy, pressure and viscosity reported in Table 1 represent the averaged errors of the 2 independent nonequilibrium trajectories. The data include calculations with the two-body potential alone and the combined two-body + AT potential. These results, and various attempts to fit the simulation data, are illustrated in Figures 1 - 4.

Earlier work [1] for argon indicates that both the pressure and energy varies linearly with the square of the strain rate. In Figures 1(a), and 1(b), energy and pressure, respectively are illustrated as functions of the square of the stain rate. In all cases there is clearly a linear relationship with the square of the strain rate. An accurate straight line equation can be obtained from a least squares fit of the simulation data. The coefficients for the straight line fits are summarised in Table 2. Table 2 also includes

data for the average absolute deviation (AAD) [24], which is a measure of how accurately the fitted equations can reproduce all of the simulation data. We observe that the percentage AAD is small, indicating that the strain rate squared relationships can accurately reproduce the simulation data.

Mode-coupling theory predicts that the pressure and energy of a fluid has a linear dependence with strain rate raised the power of three-halves. To test this hypothesis, we plot the energy (Figure 2(a)) and pressure (Figure 2(b)) of the fluid against strain rate raised to the power of three-halves. It is apparent that there are considerable deviations from linearity for pressure whereas the relationship appears linear for energy.

The difference in the quality of agreement between the alternative fits is evident by the AAD obtained (Table 2). In contrast to the strain rate-squared case, attempting to fit pressure to a linear relationship involving strain rate to the power of three-halves, results in a four-fold increase in the AAD. Although, in both cases, the percentage AADs for the energy comparisons are small, the discrepancy reported for the three-halves fit is twice the discrepancy obtained using the strain rate-squared fit. Comparison of Figure 1 with Figure 2 and the AADs reported in Table 2 for the different fits, clearly indicates that the stain rate-squared relationship is the superior alternative for both energy and pressure.

The strain rate-squared dependence is caused primarily by the two-body potential. For example, in Figure 3, the two-body and two-body + three-body, contributions to pressure are illustrated separately as a function of the square of the strain rate. It is evident that the effect of the three-body term is to shift the pressure to higher values. A similar effect is observed for both viscosity and energy.

In Figure 4, a comparison is given of viscosity as a function of strain rate. We have attempted to fit the data to linear relationships involving strain rate to the power of a half, one, three-halves and two. All of these relationships yield results of approximately similar quality as indicated by the AADs summarised in Table 2. This is consistent with results reported [1] for argon. The inability to unequivocally determine a unique linear dependence can be partly attributed to the well-known observation that viscosity is strain rate independent for low strain rates.

We are aware that there are several factors that can lead to erroneous results. Therefore as detailed extensively elsewhere [1], we applied several tests. To check that there was no error in the evaluation of the pressure tensor, we calculated the pressure tensor by another independent method, namely by integrating over the total nonequilibrium pair distribution function. The results from the two approaches were identical. To ensure that the SLLOD algorithm was correctly implemented, and that the pressures and shear stresses were correctly calculated we also checked that the energy dissipation was given correctly. Additionally, we checked that the hydrostatic pressure calculation was correct by calculating the dissipation for a fluid undergoing planar elongation [25]. A further complication at relatively high stain rates is the onset of string phases. We took three-dimensional snapshots of the configuration at arbitrary times to satisfy ourselves that no string phases were formed for the strain rates used here.

4. Conclusions

NEMD simulations are reported for the shear viscosity of xenon using accurate intermolecular two-body and three-body potentials. The data indicates that both the

pressure and energy of the fluid vary linearly with the square of the strain rate. This is consistent with earlier work [1] for the strain rate dependency of argon.

Acknowledgements

GM thanks the Australian government for an International Postgraduate Research Award (IPRA). Generous allocations of computer time on the Fujitsu VPP300 and NEC Sx-4/32 computers were provided by the Australian National University Supercomputer Centre and the CSIRO High Performance Computing and Communications Centre, respectively.

References

[1] G. Marcelli, B. D. Todd and R. J. Sadus, Phys. Rev. E., 2000, submitted.

[2] J.A. Barker, R.A. Fisher, and R.O. Watts, Mol. Phys., 21 (1971) 657.

[3] B.M. Axilrod and E. Teller, J. Chem. Phys., 11 (1943) 299.

[4] K. Kawasaki and J.D. Gunton, Phys. Rev. A, 8 (1973) 2048.

[5] D.J. Evans, Phys. Rev. A, 22 (1980) 290.

[6] D.J. Evans, Phys. Rev. A, 23 (1981) 1988.

[7] S. Sarman, D. J. Evans and P. T. Cummings, Phys. Rep., 305 (1998) 1.

[8] S.H. Lee and P.T. Cummings, J. Chem. Phys.**,** 99 (1993) 3919.

[9] S.H. Lee and P.T. Cummings, J. Chem. Phys., 101 (1994) 6206.

[10] J.-P. Ryckaert, A. Bellemans, G. Ciccotti, and G.V. Paolini, Phys. Rev. Lett., 60 (1988) 128.

[11] K.P. Travis, D.J. Searles, and D.J. Evans, Mol. Phys.**,** 95 (1998) 195.

[12] D.J. Evans and G.P. Morriss, Statistical Mechanics of Nonequilibrium Liquids, Academic Press, London, 1990.

[13] D.J. Evans, S.T. Cui, H.J.M. Hanley and G.C. Straty, Phys. Rev. A, 46 (1992) 6731.

[14] J. A. Barker, R. O. Watts, J. K. Lee, T. P. Schafer, and Y. T. Lee, J. Chem. Phys., 61 (1974) 3081.

[15] P. J. Leonard and J. A. Barker, in Theoretical Chemistry: Advances and Perspectives Vol. 1., edited by H. Eyring and D. Henderson, Academic, London, 1975.

[16] G. C. Maitland, M. Rigby, E. B. Smith and W. A. Wakeham, Intermolecular Forces, Their Origin and Determination, Clarendon, Oxford, 1981.

[17] R. J. Sadus, Molecular Simulation of Fluids: Theory, Algorithms and Object-Orientation, Elsevier, Amsterdam, 1999.

[18] G. Marcelli and R. J. Sadus, J. Chem. Phys., 111 (1999) 1533.

[19] M. A. van der Hoef and P. A. Madden, J. Chem. Phys., 111 (1999) 1520.

[20] G. Marcelli and R. J. Sadus, J. Chem. Phys., 112, (2000) 6382.

[21] J.H. Irving and J.G. Kirkwood, J. Chem. Phys., 18 (1950) 817.

[22] C. W. Gear, Numerical Initial Value Problems in Ordinary Differential Equations, Prentice-Hall, Englewood Cliffs, NJ, 1971.

[23] P. Attard, Phys. Rev. A., 45 (1992) 5649.

[24] R. J. Sadus, J. Phys. Chem., 99 (1995) 12363.

[25] B.D. Todd, Phys. Rev. E, 56 (1997) 6723.

Table 1. Molecular simulation data for the pressure, energy and viscosity obtained at different strain rates using the two-body potential of Barker et al. [14] alone and in conjunction with the three-body Axilrod-Teller [3] potential.

	two-body potential only			two-body + three-body potential		
$\dot{\gamma}$	P	E_{conf}	η	P	E_{conf}	η
0.2	-0.156(6)	-3.672(4)	0.77(1)	0.0150(1)	-3.509(1)	0.76(1)
0.4	-0.152(5)	-3.688(2)	0.772(3)	0.0243(9)	-3.5022(4)	0.765(2)
0.6	-0.138(2)	-3.683(5)	0.758(4)	0.0387(2)	-3.4938(1)	0.749(1)
0.8	-0.1187(8)	-3.660(1)	0.753(4)	0.065(1)	-3.4795(6)	0.739(1)
1	-0.088(6)	-3.6354(7)	0.7438(7)	0.092(2)	-3.4628(8)	0.7263(8)
1.2	-0.0527(1)	-3.611(2)	0.733(2)	0.132(3)	-3.443(3)	0.716(2)
1.4	-0.0073(9)	-3.5875(5)	0.717(1)	0.184(4)	-3.4211(1)	0.706(1)
1.6	0.046(3)	-3.5577(4)	0.7021(3)	0.237(1)	-3.395(1)	0.6892(7)
1.8	0.1073(6)	-3.5304(6)	0.6882(9)	0.298(1)	-3.3689(3)	0.6789(8)

Table 2. Summary of the various strain rate-dependent fits for pressure, energy and viscosity with their absolute average deviations (AAD).

Fitting Equation	a	b	AAD (%)
$P = a + b\dot{\gamma}^{3/2}$	0.0027(1)	0.1054(3)	16.04
$P = a + b\dot{\gamma}^{2}$	0.0108(1)	0.0868(3)	3.49
$E = a + b\dot{\gamma}^{3/2}$	-3.5224(1)	0.0616(1)	0.08
$E = a + b\dot{\gamma}^{2}$	-3.5094(1)	0.0447(1)	0.04
$\eta = a + b\dot{\gamma}^{1/2}$	0.849(2)	-0.125(2)	0.86
$\eta = a + b\dot{\gamma}$	0.7863(2)	-0.0598(8)	0.38
$\eta = a + b\dot{\gamma}^{3/2}$	0.7654(8)	-0.0367(5)	0.31
$\eta = a + b\dot{\gamma}^{2}$	0.7549(7)	-0.0247(3)	0.57

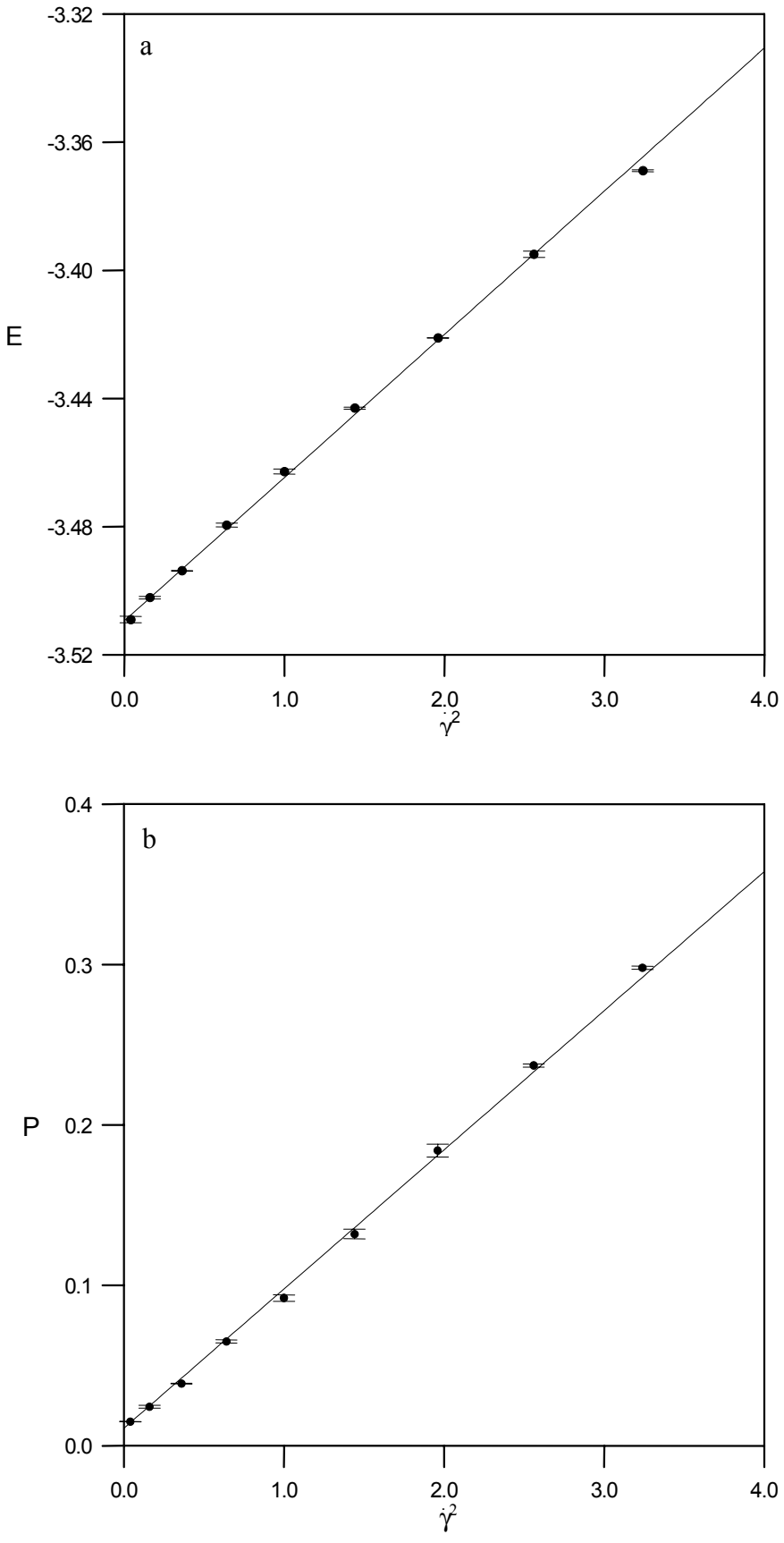

Fig. 1 Molecular simulation data (•) for (a) energy and (b) pressure as a function of the strain rate-squared. The lines represent the linear fits summarised in Table 2.

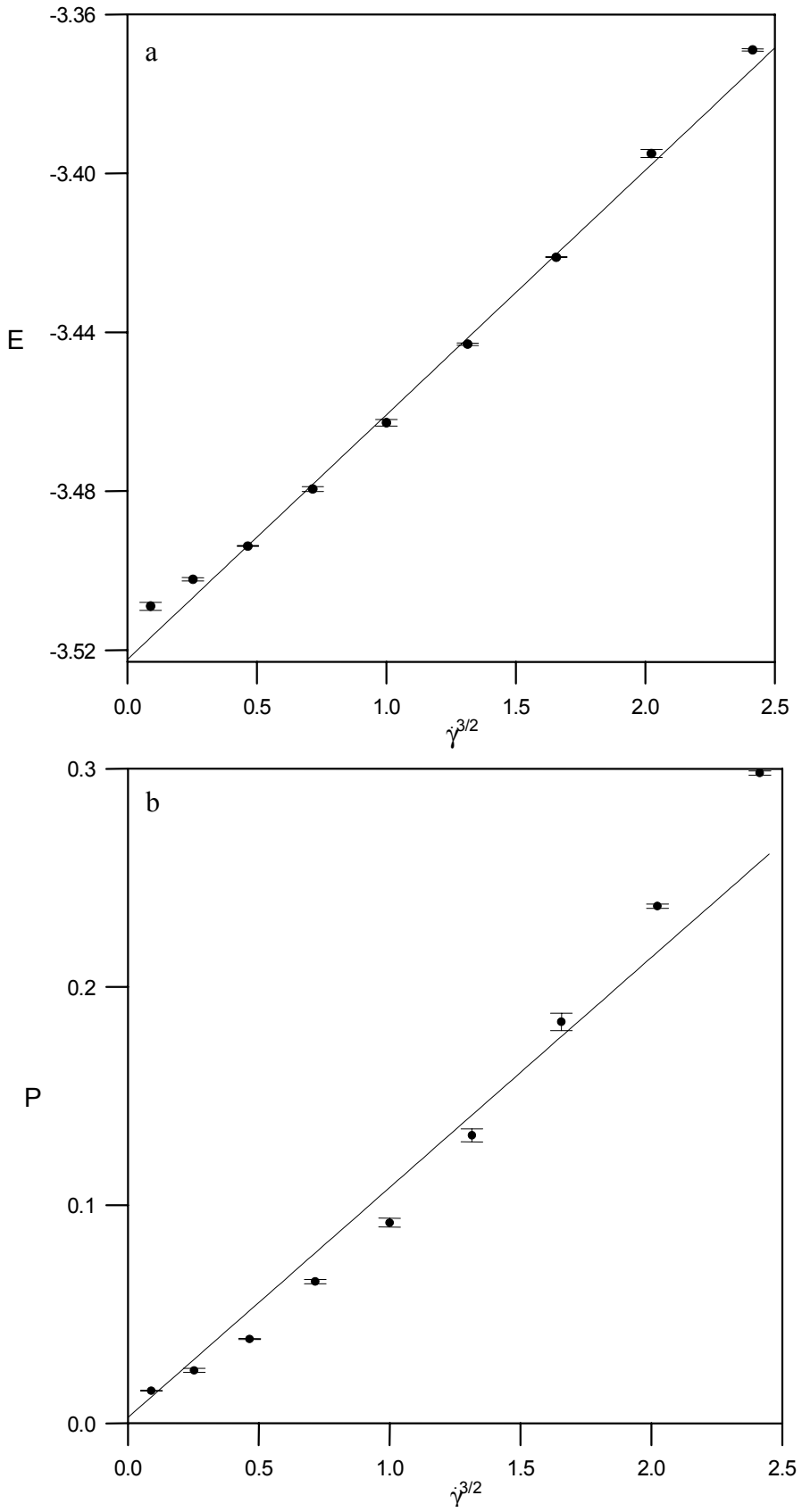

Fig. 2 Molecular simulation data (•) for (a) energy and (b) pressure as a function of the strain rate to the power of three-halves. The lines represent the linear fits summarised in Table 2.

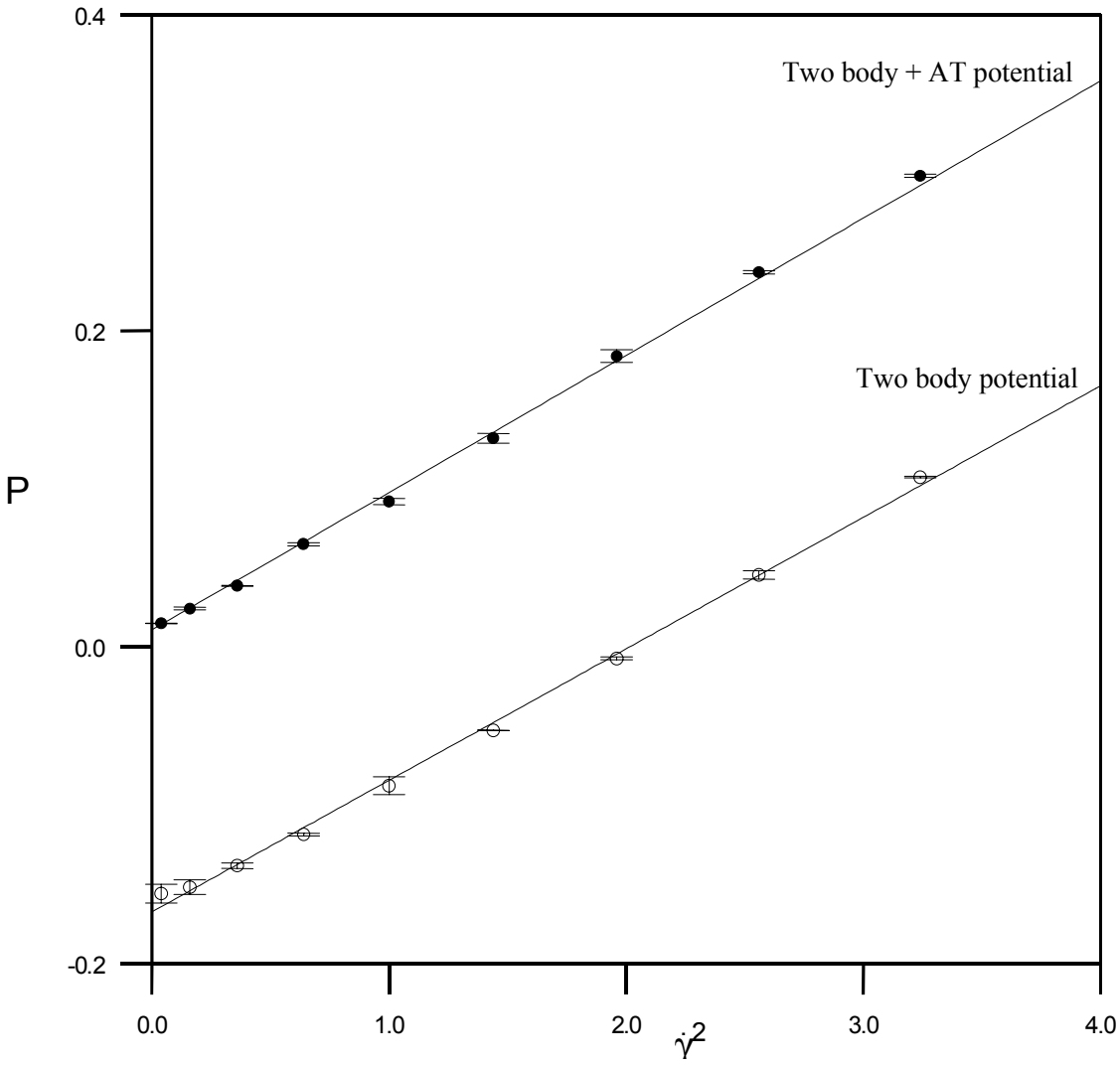

Fig. 3. Comparison of the contribution to pressure of the two-body + AT potential (•) and the two-body only (O) potential.

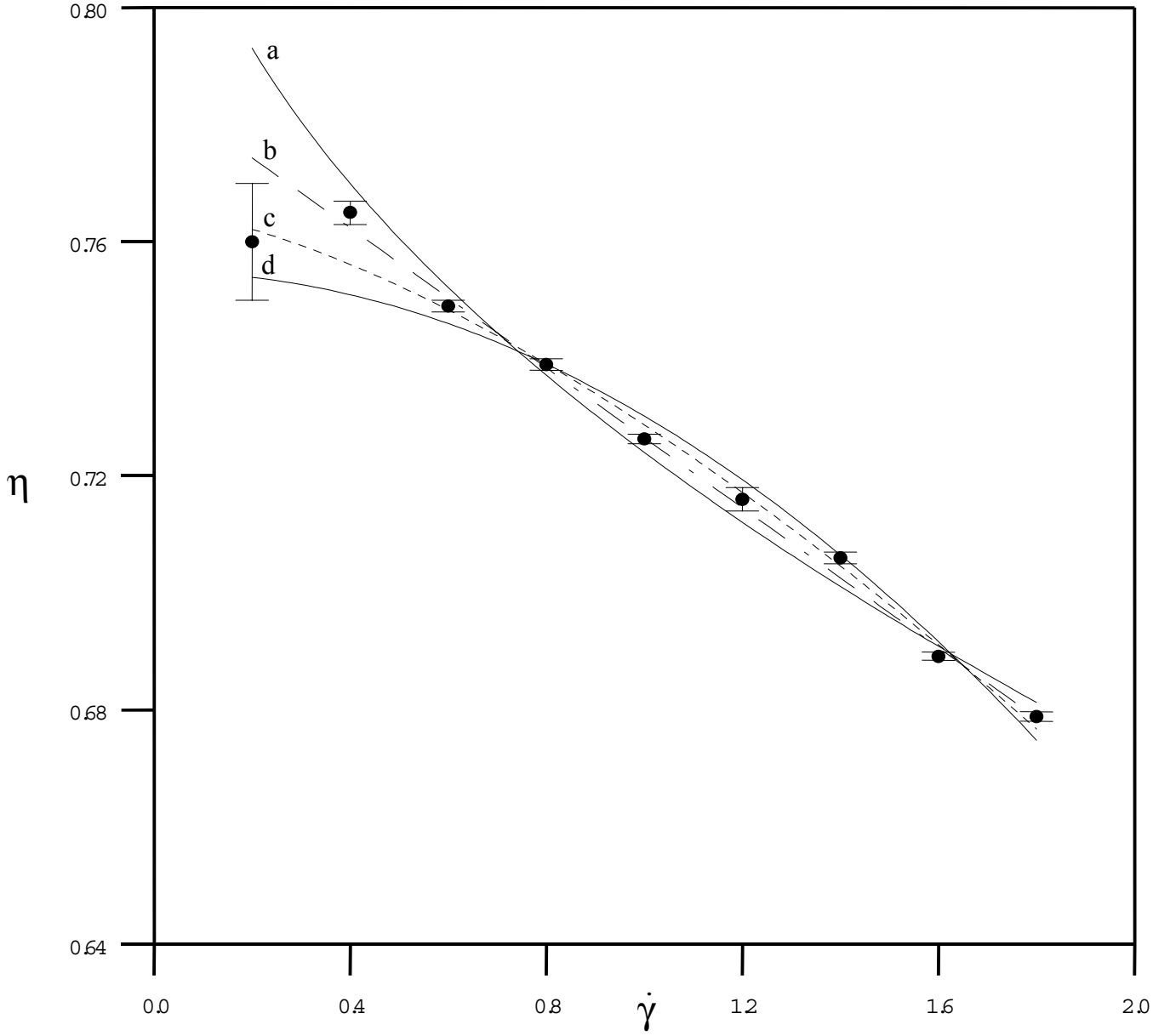

Fig. 4. Molecular simulation data for viscosity as a function of the stain rate. The lines illustrate different fits with a strain rate dependency to the power of (a) ½, (b) 1, (c) 3/2 and (d) 2. The parameters for these fits are summarised in Table 2.